



Tailoring Microstructure of Silica Xerogels via a Facile Synthesis Approach

Suh Cem Pang, Sze Yun Kho, Suk Fun Chin

*Department of Chemistry, Faculty of Resource Science and Technology,
Universiti Malaysia Sarawak, 94300, Kota Samarahan, Sarawak, Malaysia.*

Received 27 Feb 2013, Revised 24 Mar 2013, Accepted 24 Mar 2013

*Corresponding author. Email: suhcem@gmail.com

Abstract

Silica xerogels of tailored microstructure were prepared via a facile synthesis approach. This approach entails the preparation of silica nanoparticles using the sol-gel method under the influence of low frequency ultrasonication. By applying optimum synthesis conditions, silica nanoparticles of tailored mean sizes in the form of silica sol type B (158.3 ± 14.1 nm), and silica sol type M (83.1 ± 22.5 nm) were successfully synthesized. The various mean particle sizes were then mixed in predetermined molar ratios, and subsequently gelation under controlled conditions. The effect of adding polyvinyl pyrrolidone (PVP) as a polymeric surfactant on the microstructure of silica xerogels was also investigated.

Keywords: silica xerogels, mean particle size, surfactant

1. Introduction

Nanomaterials of substantially enhanced properties over their bulk counterparts have led to intensified research interest and increased industrial demands in recent years. Silica-based nanomaterials such as silica nanoparticles and xerogels have been extensively studied by scientists worldwide due to their ease of preparation and numerous potential applications. Silica nanoparticles possess superior properties such as adjustable refractive index, high porosity, low thermal conductivity and low dielectric constant. They are widely being used in various applications including catalysis [1-2], drugs delivery [3-4], thin-film substrates [5], corrosion protection [6], stabilizers [7], humidity sensors [8] and optical sensors [9]. Silica nanoparticles are mainly synthesized by the sol-gel process [10-12] and water-in-oil emulsion [13]. The mean sizes of silica nanoparticles can be easily controlled by varying the synthesis parameters, such as the reaction temperature [11], aging duration and conditions [14], washing solvent [15] and drying conditions [14, 16]. Since the discovery of surfactant-templated mesoporous silica in 1992 [17], studies on microstructural control of silica had been carried out extensively. However, the removal of template from synthesized silica literally created problems. For example, mesoporous molecular sieves of MCM-48 were usually synthesized in basic conditions by self-assembly, using tetraethylorthosilicate (TEOS) as the silica source and cetyltrimethylammonium bromide (CTAB) as the template which was eventually removed by calcination. Calcination is a process of decomposing the organic template into carbon dioxide and organic amine compounds [18]. The pore diameters decreased as a result of silica lattice shrunk during calcination. Besides that, silica xerogels were also synthesized by the acidification of sodium silicate using hydrochloric acid and acetic acid via a sol-gel process. The microstructure of resulting silica xerogels were affected by the concentration of acetic acid used [19].

In this study, preformed silica nanoparticles of different mean sizes were used to prepare silica xerogels of desired microstructure. Two different types of silica sols were prepared: silica nanoparticles of mean diameter 158.3 ± 14.1 nm (designated as Type B), and silica nanoparticles of mean diameter 83.1 ± 22.5 nm (designated as Type M). Silica sols of both Type B and Type M were used for preparing silica xerogels. The effect of varying molar ratios of Type B and Type M of silica sols on the microstructure and surface morphology of silica xerogels formed were investigated. Besides, effect of adding a polymeric surfactant polyvinyl pyrrolidone (PVP), on the resulting microstructure of silica xerogels was investigated.

2. Materials and Methods

2.1. Materials

Tetraethylorthosilicate, TEOS (99.3%, J.T. Baker), absolute ethanol (99.0%, HmBG Chemicals), ammonia solution, NH_4OH (28%, R & M Chemicals), Polyvinyl pyrrolidone, PVP (Avocado) and Ultrapure water (18.2 M Ω) obtained from a water purification system (Elga PURELAB Ultrapure Water System) were used throughout the study. All chemicals were used as received without any purification.

2.2. Preparation of silica sols

Silica sols of mean particle size ranges 158.3 ± 14.1 nm (Type B) were synthesized by hydrolysis and condensation of TEOS at predetermined molar ratios of $[\text{H}_2\text{O}]/[\text{TEOS}]$ of 85:1 in mixtures of absolute ethanol and ultrapure water based on a reported synthesis method [11]. Firstly, predetermined volumes of absolute ethanol and water were mixed in a sonication bath for 10 minutes. A known volume of TEOS was then added to the mixture while sonicating. After mixing for 20 minutes, a fixed amount of NH_4OH was added as a catalyst to promote the condensation reaction. The molar ratios of $[\text{NH}_4\text{OH}]/[\text{TEOS}]$ was fixed at 4:1. Sonication was continued for a further 60 minutes to ensure the completion of hydrolysis and condensation reactions. All experiments were conducted at room temperature of 25°C. The same synthesis procedure as mentioned above was repeated for preparing silica sols of mean particle size ranges 83.1 ± 22.5 nm (Type M).

2.3. Preparation of silica xerogels

Silica sols of Type B and Type M were used to prepare silica sol mixtures at various predetermined molar ratios as shown in Table 1. All sol mixtures were sonicated for 30 minutes to ensure homogenous mixing. In separate experiments, various known amounts of PVP were added to samples of Type B silica sol to study the effect of polymeric surfactant on the microstructure of silica xerogels (Table 2). All xerogel samples were obtained by keeping the sol mixtures in an oven at 60°C for 24 hours.

Table 1: Composition of silica sol mixture of different mean particle sizes

Designated sample code	Mole ratio	
	Sol B	Sol M
BM11	1	1
BM13	1	3
BM31	3	1
BM16	1	6
BM61	6	1

Table 2: Composition of silica sol Type B with different amount of PVP

Designated sample code	Percentage (wt %) of PVP
PVP001	0.01
PVP005	0.05
PVP010	0.10

2.4. Characterization of silica nanoparticles and xerogels

The morphology and mean particle size of silica nanoparticles were characterized by Scanning Electron Microscopy (SEM) (JEOL Model JSM-5300LV) at various magnifications. Pre-cleaned stainless steel plates were used as supporting substrates for all silica samples. The mean particle size of silica nanoparticles was calculated from the diameters of 300 nanoparticles as observed in SEM micrographs using Smile View software.

The microstructural characterization of silica xerogel samples were carried out using a Brunauer-Emmett-Teller (BET) surface area analyzer (Micromeritics ASAP 2010) at 77K. Nitrogen adsorption-desorption isotherms over a range of relative pressure (P/P_0) from 0.05 to 1.00 were collected for all samples. Specific surface areas were determined from the BET equation at a relative pressure range between 0.05 to 0.30.

3. Results and Discussion

3.1 Microstructural characterization of silica xerogels

Figure 1 shows FESEM micrographs of silica xerogels prepared from silica sols of Type B and Type M with mean particle sizes of 158.3 ± 14.1 nm and 83.1 ± 22.5 nm, respectively. Both silica xerogels of Type B and M exhibited Type IV isotherm with H1 hysteresis loop according to the International Union of Pure and Applied Chemistry (IUPAC) classification (Figure 2) which is characteristic of mesoporous solids [21]. According to IUPAC, pores are being classified into three types: micropores (diameter below 2 nm), mesopores (diameter greater than 2 nm and smaller than 50 nm), and macropores (diameter greater than 50 nm) [22-23]. As shown in Figure 3, silica xerogels of Type B exhibited a wide range of pore sizes with pore diameters ranged between 2 nm and more than 80nm, with macropores contributed more than 90% of its total pore volume. In contrast, silica xerogels of Type M showed a substantially narrower range of pore sizes between 3 nm and 16 nm with its dominant pore diameter occurred at about 5 nm. Besides, the total pore volume of Type M silica xerogel was substantially lower than that of Type B silica xerogel.

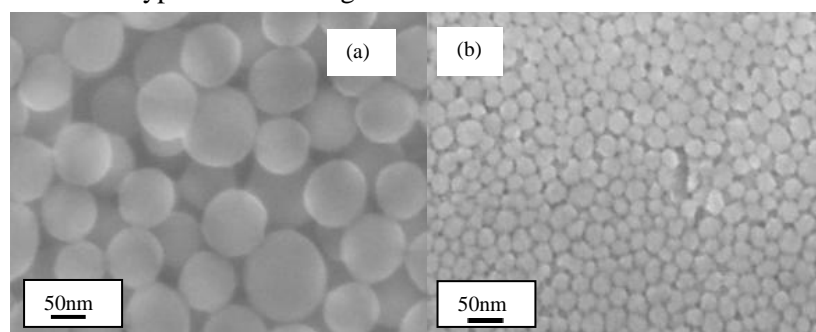


Figure 1: FESEM micrographs of silica xerogels of (a) Type B, and (b) Type M

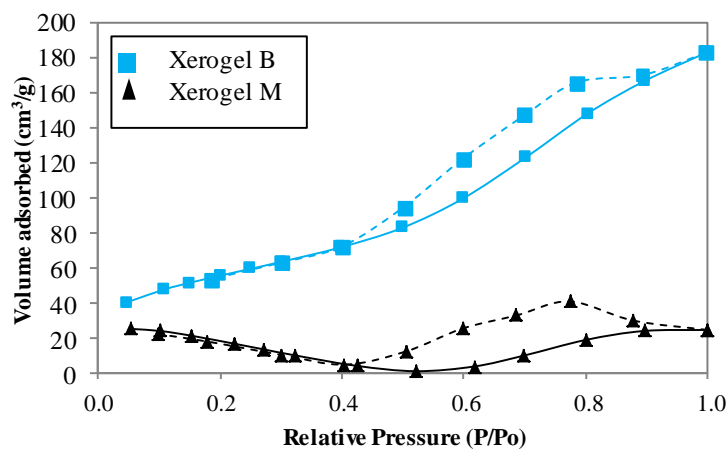


Figure 2: Nitrogen adsorption (solid line)-desorption (dashed line) isotherms of silica xerogels of Type B and Type M

3.2 Microstructural control of silica xerogels

The microstructure of silica xerogels was varied and tailored by mixing of silica sols of Type B and Type M at predetermined molar ratios, and subsequently underwent controlled gelation. Figure 4 shows SEM micrographs of silica xerogels prepared from mixtures of silica sols Type B and Type M at various molar ratios. These silica xerogels were observed to exhibit different surface morphology due to different patterns of nanoparticle arrangements based upon the relative ratios of Type B and Type M silica nanoparticles present. The mean particle sizes of these xerogel samples were within size ranges of their respective parental sols of between 80 nm and 160 nm (Table 3). For instance, BM11 xerogel which consisted of equal amount of Type B and Type M silica sols exhibited a mean particle sizes of 98.0 nm, whereas xerogel samples BM16 and BM61 showed mean particle sizes of 89.0 nm and 104.0 nm, respectively. In general, relatively higher mean particle sizes were observed in xerogel samples which consisted of higher molar ratios of Type B silica sol.

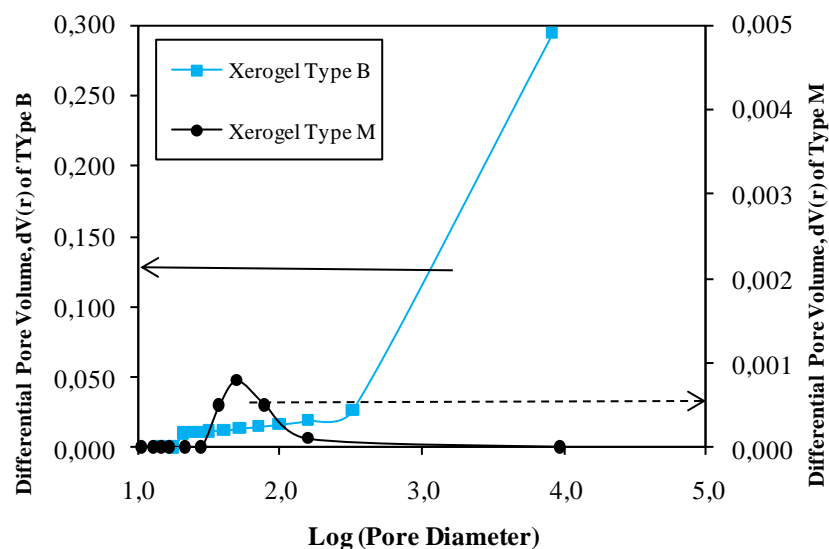


Figure 3: Pore size distribution of silica xerogels of Type B and Type M. (Note the different vertical axis scales)

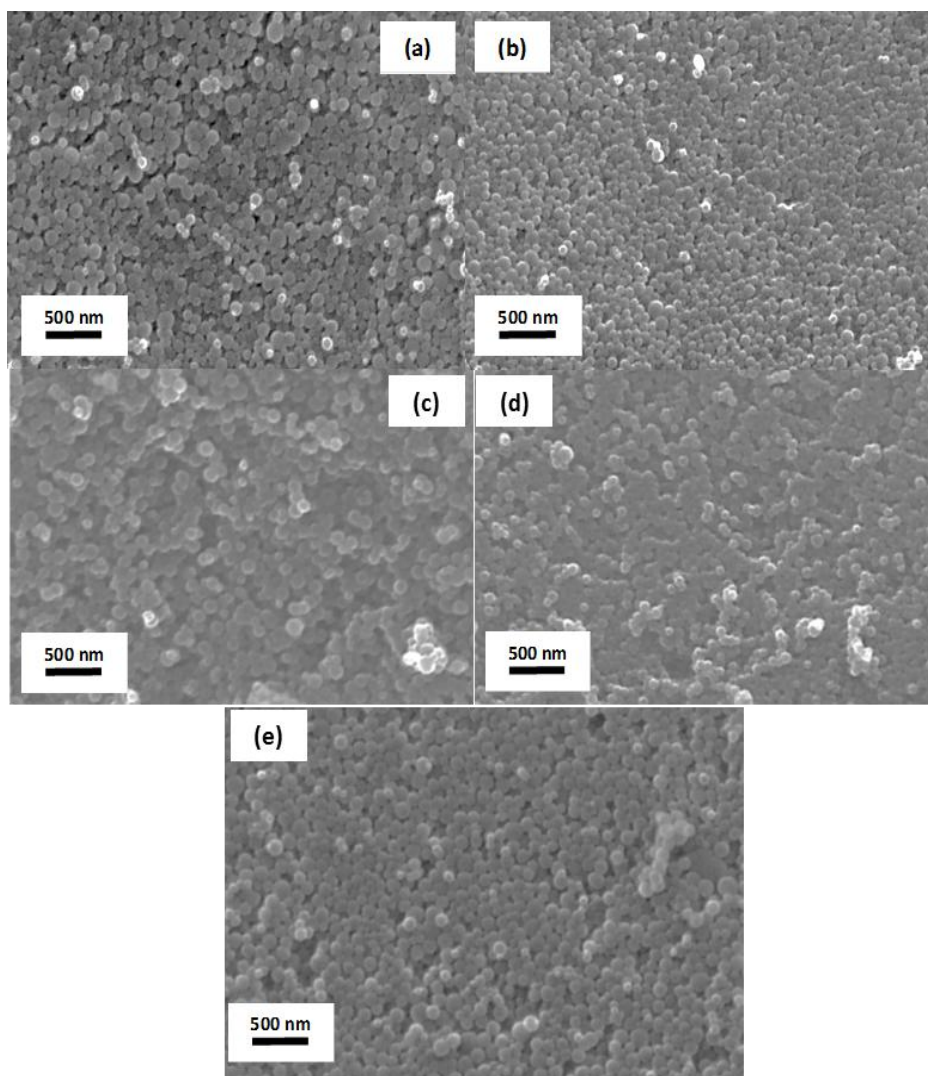


Figure 4: SEM micrographs of silica xerogels (a) BM11, (b) BM13, (c) BM31, (d) BM16, and (e) BM61

Table 3: Mean particle sizes of xerogel samples prepared from mixtures of silica sols of Type B and Type M

Designated xerogel sample	Mixture of silica sol of Types B & M (molar ratio)	Mean particle size (nm)
BM11	1:1	98.0
BM13	1:3	88.5
BM31	3:1	98.0
BM16	1:6	89.0
BM61	6:1	104.0

Figures 5 and 6 show the comparison of pore size distribution for silica xerogels prepared by mixing silica sols of Types B and Type M at various molar ratios. It was evident that the mixing of Type B and Type M silica sols could substantially influence the pore size distribution of silica xerogels formed. The observed shift in the pore size distribution indicated that silica xerogel samples changed progressively from macroporous to mesoporous in the presence of higher proportion of Type M nanoparticles relative to Type B nanoparticles (Figure 5). Such microstructural changes could be attributed to the higher packing density inherent of smaller Type M silica nanoparticles. Besides, coarse pores or interstitial spaces formed between Type B nanoparticles could be readily filled up by Type M nanoparticles thereby resulting in higher packing density and the generation of smaller pores. Furthermore, the total pore volume of silica xerogels was observed to have increased substantially, indicating an increase in the overall porosity of the xerogels sample in the presence of higher proportion of Type M silica nanoparticles. In contrast, increasing the proportion of Type B nanoparticles relative to Type M nanoparticles (e.g. sample BM61, Figure 6) did not appear to have any substantial effect on the total pore volume or overall porosity of the silica xerogels formed. However, silica xerogels exhibited narrower ranges of pore size distribution indicating the formation of more uniform pore sizes in the presence of higher proportion of larger sized silica nanoparticles.

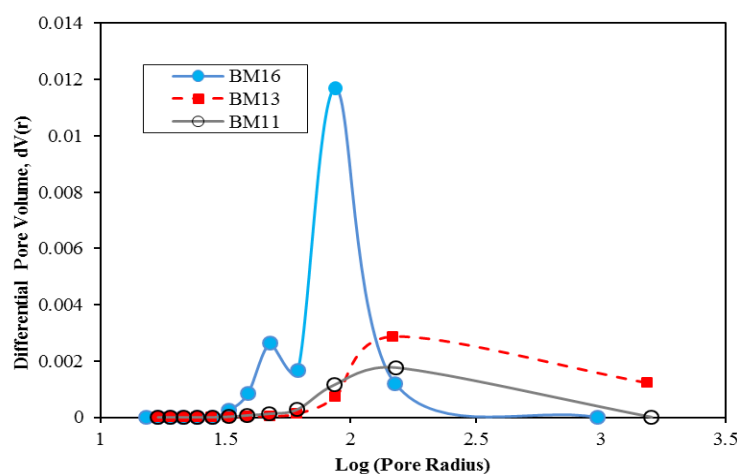


Figure 5: Pore size distribution of silica xerogel samples prepared with mixtures of Type B and Type M silica sols at molar ratios of 1:1, 1:3 and 1:6

The plausibility of microstructural control of silica xerogels through direct mixing of predetermined molar ratios of silica nanoparticles of different mean sizes was further investigated and was shown in Figures 7 and 8. The molar ratio of Type B and Type M silica nanoparticles appeared to have substantial effect on the surface area distribution as indicated by the shift of dominant pore sizes within these silica xerogels. Surface area contribution by smaller pore sizes appeared to dominate in the presence of higher proportion of Type M silica nanoparticles (Figure 7). This observation is in consonance with earlier contention that the overall porosity of silica xerogels had increased substantially in the presence of higher proportion of Type M silica nanoparticles, which in turn, contributed to the higher surface area. In contrast, increased molar ratio of Type B silica nanoparticles did not lead to any notable increase in the overall surface area of silica xerogel formed (Figure 8). In these cases, the total surface area was attributed mainly to the presence of dominant pore sizes within these silica xerogels.

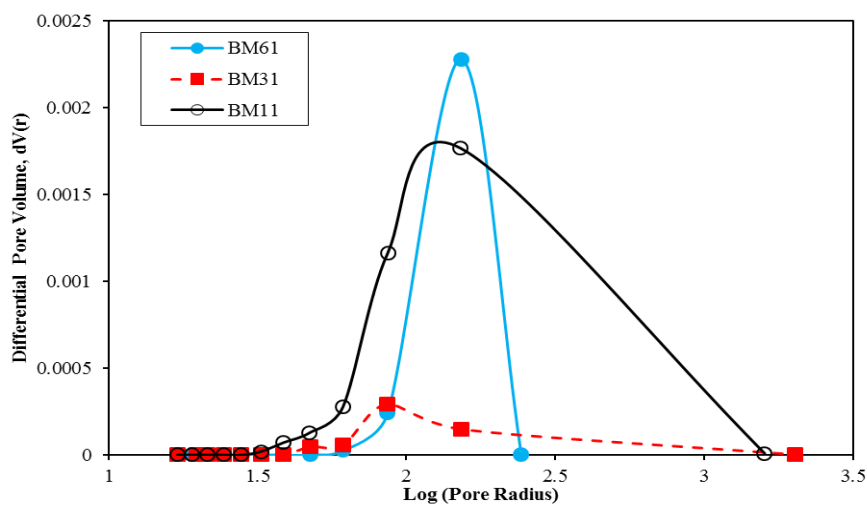


Figure 6: Pore size distribution of silica xerogels samples prepared with mixtures of silica Type B and Type M sols at molar ratios of 1:1, 3:1 and 6:1

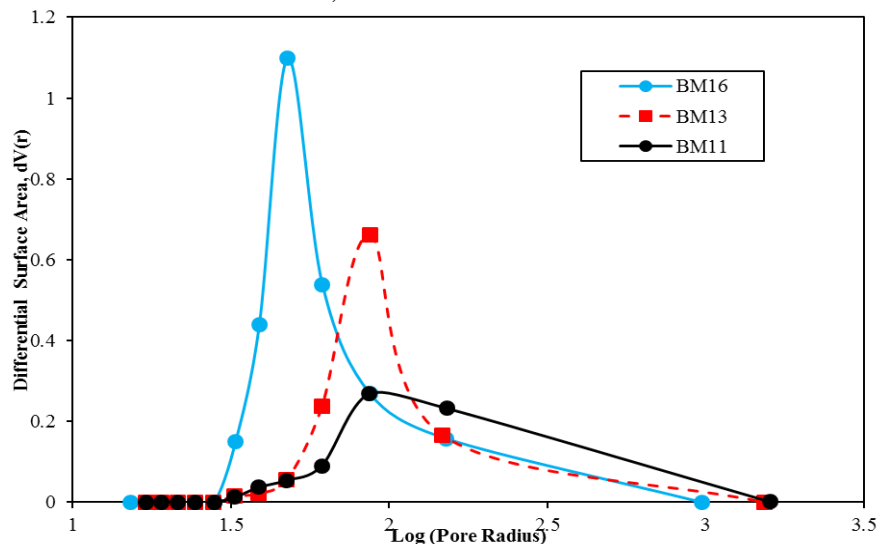


Figure 7: Surface area distribution of silica xerogel samples prepared with mixtures of silica Type B and Type M sols at molar ratios of 1:1, 1:3 and 1:6

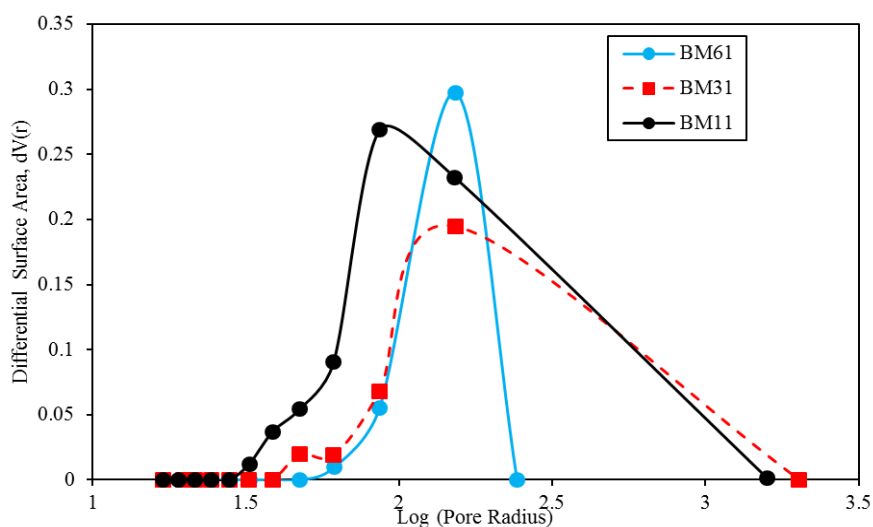


Figure 8: Surface area distribution of silica xerogel samples prepared with mixtures of silica Type B and Type M sols at molar ratios of 1:1, 3:1 and 6:1

3.3 Effect of polymeric surfactant

The effect of polymeric surfactant on the microstructure of silica xerogels was investigated by adding known amounts of PVP into Type B silica sol. Table 3 shows a comparison of the microstructural characteristics of various silica xerogel samples formed without and in the presence of 0.01 to 0.1 wt.% of PVP polymeric surfactants.

Silica xerogel samples exhibited substantially higher specific surface area with the addition of 0.01 and 0.05 wt.% PVP (Sample designated as PVP0.01 and PVP0.05 respectively). Silica xerogel prepared with the addition of 0.05 wt.% PVP exhibited the highest specific surface area of about 125 cm²/g which was several times higher than silica xerogels without addition of any surfactant (~23 cm²/g). Such substantial increase in surface area could be attributed to an overall increase in the porosity associated with increased total pore volume (Table 4). PVP served as a surfactant to prevent silica nanoparticles aggregation and hence more open pores were created during gelation.

Table 4: Comparison of specific surface area (m²/g), total pore volume (cm³/g) and pore diameter (nm) of different silica xerogel samples

Xerogel sample	Specific surface area ^a (m ² /g)	Total pore volume ^b (cm ³ /g)	Average pore diameter (nm)	Average pore diameter (nm)
B	23.3	0.0078	0.70	158.3
M	29.5	0.0377	2.56	83.1
PVP0.01	57.3	0.0188	0.65	158.3
PVP0.05	125.4	0.3563	5.68	158.3
PVP0.10	23.1	0.0227	1.96	158.3

^aBy BET equation; ^bAt P/Po= 0.99; PVP 0.01 denotes xerogel sample with 0.01 wt % PVP added

Silica xerogels of tailored microstructure possess numerous potential applications. Mesoporous silica nanoparticles of mean diameter less than 300 nm and of mean pore size 2 nm pores are suitable for biomedical applications such as gene transfection reagents, cell markers and carriers of molecules [4]. Angelos *et al.* reported that mesoporous silica nanoparticles functionalized with biocompatible nano impellers and nano valves were promising materials for on-demand release of a wide range of drug molecules [4]. Colomer *et al.* reported the preparation of mesoporous silica xerogels with a pore volume of 0.45 ± 0.01 cm³/g and mean pore size of 3.7 nm which could potentially be used as proton exchange membranes in fuel cells [23]. Our current research findings have set the stage for further development and optimization of synthesis approaches for the preparation of silica xerogels with tailored microstructure.

Conclusion

We have demonstrated the plausibility of preparing silica xerogels with tailored microstructures via a facile and cost-effective approach. Such microstructural control could be achieved by controlled mixing of preformed silica nanoparticles of different mean sizes at predetermined molar ratios, or by the addition of an appropriate polymeric surfactant prior to gelation under controlled conditions. It is envisaged that further development and optimization of the synthesis approaches for the preparation of silica xerogels with tailored microstructure should lead to more potential applications in many technological and biomedical fields.

Acknowledgment

The authors acknowledge financial supports rendered through the award of research grants by Universiti Malaysia Sarawak (UNIMAS) under the special fundamental Research Grant 01(K03)/557/2005(56).

Reference

1. Johnson B.F.G., Raynor S.A., Brown D.B., Shephard D.S., Mashmeyer T., Thomas J.M., Hermans S., Raja R., Sankar, G., *J. Mol. Catal. A: Chem.*, 182-18 (2002) 89-87.
2. Taguchi A., Schüth F., *Microporous Mesoporous Mater.*, 77 (2005) 1-45.
3. Lopéz, T., Quintana, P., Martínez, J.M., Esquivel, D., *J. Non-Cryst. Solids*, 353 (2007) 987-989.
4. Angelos, S., Liong, M., Choi, E., Zink, J.I., *Chem. Eng. J.*, 137 (2008) 4-13.
5. Wang, C.T. and Wu, C.L., *Thin Solid Films*, 496 (2006) 658-664.

6. Pepe A., Galliano P., Aparicio M., Durán A., Ceré S., *Surf. Coat. Technol.*, 200 (2006) 3486-3491.
7. Ruliko Y., Suzuki S., Shirai K., Yamauchi T., Tsubokawa N., Tsuchimochi M., *Eur. Polym. J.*, 42 (2006) 221.
8. Lee C.W., Park H.S., Kim J.G., Choi B.K., Joo S.W., Gong M.S., *Sens. Actuators, B*, 109- (2005) 315-322.
9. Estella J., Echeverría J.C., Laguna M., Garrido J.J., *J. Non-Cryst. Solids*, 353-2 (2007) 286-294.
10. McDonagh C., Sheridan F., Butler T., MacCraith, B.D., *J. Non-Cryst. Solids*, 194 (1996) 72-77.
11. Rao K.S., El-Hami K., Kodaki T., Matsushige K., Makino K., *J. Colloid Interface Sci.*, 289 (2005) 125-131.
12. Baccile N., Babonneau F., Thomas B., Coradin T., *J. Mater. Chem.*, 19 (2009) 8537-85596.
13. Arbakan I., Doussineau T., Smaïhi M., *Polyhedron*, 25 (2006) 1763-1770.
14. Estella J., Echeverría J.C., Laguna M., Garrido J.J., *Microporous Mesoporous Mater.*, 102 (2007) 274-282.
15. Fidalgo, A., Ilharco, L.M. *Microporous Mesoporous Mater.*, 4(2005)229-235.
16. Rahman, I.A., Vejayakumaran, P., Sipaut, C.S., Ismail, J., Bakar, M.A., Adnan, R., Chee, C.K., *Colloids Surf. A: Physicochem Eng. Asp.*, 294 (2007) 102-110.
17. Kresge, C.T., Leonowicz, M.E., Roth, W.J., Vartuli, J.C., Beck, J.S., *Nature*, 359 (1992) 710-712
18. Ji H., Fan Y., Jin W., Chen C., Xu N., *J. Non-Cryst. Solids*, 354 (2008) 2010-2016.
19. Witoon T., Tatan N., Rattanaichian P., Chareonpanich M. *Ceram. Int.*, 37 (2011) 2297.
20. Xu Y., Zhang B., Fan W.H., Wu D., Sun Y.H., *Thin Solid Films*, 440 (2003) 180-183.
21. Sing K.S.W., Everett, D.H., Haul R.A.W., Moscou L., Pierotti, R.A., Rouquerol J., Siemieniewska T., *Pure Appl. Chem.*, 57 (1985) 603-619.
22. Rouquerol J., Avnir D., Fairbridge C.W., Everett, D.H., Hayness J.H., Pernicone N., Ramsay J.D.F., Sing K.S.W., Unger K.K., *Pure Appl. Chem.*, 66 (1994) 1739-1758.
23. Colomer M.T., Rubio F., Jurado J.R., *J. Power Sources*, 167 (2007) 53-57.

(2013); <http://www.jmaterenvironsci.com>